Characterization of spirugenic iron oxide nanoparticles and their antibacterial activity against multidrug-resistant *Helicobacter pylori*

Sherin M.A. Sharaf *, Heba S. Abbas and Tarek A.M. Ismaeil

Microbiology Department-National Organization for Drug Control and Research (NODCAR), Giza, Egypt.

Abstract:

In the present study, spirugenic iron oxide nanoparticles (SIONs) were biosynthesized using a new simple, expeditious and benign approach which was achieved by combining ferric chloride with *Spirulina platensis* water extract. SIONs were inspected using UV spectroscopy on 290nm. The Transmission Electron Microscope (TEM) recorded rod-shaped particles with an average width of 31.04 nm and length 137.51nm. X-Ray Diffractometer (XRD) showed a cubic spinel phase of γ-Fe_2O_3 (maghemite). Furthermore, SIONs exhibited good antibacterial activity against multidrug-resistant *Helicobacter pylori*. Our study demonstrated that the Minimum Inhibitory Concentration (MIC) of SIONs against multidrug resistant (MDR) *H. pylori* was 3.1 µg/ml. TEM image showed the cell rupture of *H. pylori* indicating fragmented cell membrane and leakage of bacterial components in those culture treated by SIONs. Cytotoxic activity test revealed that SIONs have no adverse effect on human epithelial cell line so it may be used safely as a natural product. The use of *S. platensis* as a nanofactory for the IONs synthesis could have a great role in the treatment of *H. pylori* infection in the future.

Keywords: *H. pylori*, Iron oxide nanoparticles, *S. platensis*, green biotechnology, antibacterial resistance.

Introduction

The references for the existence of *Helicobacter pylori* in the gastric human stomach developed an extraordinary leap in the medical conception starting from 1983 **(Li and Perez-Perez, 2018).**

H. pylori infection is responsible for diverse gastric diseases, involving gastritis, peptic ulcers, and gastric tumors **(Thamphiwatana, 2014).** The traditional medication of these infections was to give a multiple-drug regimen, such as amoxicillin, clarithromycin, furazolidone, tetracycline and metronidazole with bismuth or a proton pump inhibitor. Nevertheless, in developing nations, the

* Correspondent author: email*:* sherinashraf@yahoo.com (ISSN: 1110-8649)

evolution resistance of *H. pylori* to metronidazole and clarithromycin made the treatment difficult **(Megraud and Lehours, 2007)**. Thus, there is a demand to establish novel antibacterial approaches against *H. pylori*.

In recent years, the application of nanotechnology, especially the use of nanoparticles has generated considerable impact on medicine **(Farokhzad and Langer, 2009).** In particular, Iron Oxide Nanoparticles (IONs) have different physical and chemical properties because of electron relocation between Fe^{2+} and Fe^{3+} in octahedral sites **(Mahdavi *et al.*, 2013)**. Furthermore, their surface characteristics give its great importance in biomedical applications such as drug delivery, biological imaging, therapies **(Guoa *et al.*, 2012)**, biosensors and antimicrobial properties **(Berry and Curtis, 2003; Prabhu and Rao,2015)**.

Currently, there are several routes for the synthesis of IONs such as physical, chemical, biological routes. Chemical synthetic routes can take place via co-precipitation of aqueous ferrous and ferric solutions, microemulsion technique and hydrothermal synthesis, electrochemical deposition and sonochemical methods. Physical synthetic routes via aerosols, gas phase deposition, laser-induced pyrolysis, and powder ball mining. Also, biological methods mediated via protein, fungi, and bacteria. Diverse kinds of IONs formed using each method show specific properties. Green nanotechnology has played great attention to get rid of toxic chemicals that are harmful to the environment. Thus, there is an urgent need for the synthesis of eco-friendly IONs **(Hasany *et al.*, 2012; Devatha *et al.*, 2018).**

Cyanobacteria are a phylogenetically primeval set of Gram-negative prokaryotes that were classified for three billion years. They serve as the most archaic creatures on earth **(Sharma and Bhandari, 2006)**. *Spirulina platensis* is a cyanobacterium with economic priority as a result of protein, vitamins, essential amino acids, and fatty acid content. The biomass of *S. platensis* has been recognized to be "An amazing Food Health" because of their defined bioactive compounds such as essential fatty acids, B complex vitamin, bio-pigments, carotenoids and antioxidant compounds **(Achmadi and Tri-panji, 2000; Slonczewski *et al.*, 2009)**.

The purpose of the present study is to develop a new simple, efficient and benign synthesis method of IONs by *Spirulina platensis* to produce a spirugenic Iron oxide Nanoparticles (SIONs) using ferric chloride as iron precursor agent,

then evaluate the bactericidal effect of SIONs against multidrug-resistant (MDR)*Helicobacter pylori* as a trial for a possible future antibacterial product.

Materials and Methods

Preparation of *S. platensis* biomass

The cyanobacterium *S. platensis* was acquired from Algal Unit of National Research Center (Egypt), cultivated in Zarrouk's medium under 30±2ºC and illuminated with a white fluorescent lamp at a light intensity of 3000 Lux (16/8 h light/dark cycle). The culture was shaken thrice daily and growth performance was estimated by a spectrophotometer at 640 nm within three days interval time along 21 days **(Ahmed *et al*., 2015)**. *S. platensis* biomass harvested in the mid-exponential phase for iron oxide nanoparticles biosynthesis.

Preparation of *S. platensis* Extract

Five grams (dry weight) of *S. platensis* biomass were suspended in 100 ml of double deionized water and boiled for 15 min at 100ºC in an Erlenmeyer flask. After boiling, the mixture was cooled and centrifuged at 10000 rpm for 15 min. Water algae extract (WAE) was collected and stored at 4ºC for IONs biosynthesis **(Ali *et al*., 2015)**.

Biosynthesis of IONs

Two methods are used for IONs Biosynthesis:

The first method achieved by using one gram of wet *S. platensis* biomasses mixed with100 ml of 0.1M Ferric chloride hexahydrate ($FeCl_3.6H_2O$, 98%) for 24 h to obtain the Aqueous Algae Biomass (AAB).

In the second method water algae extract (WAE) was mixed with 0.1M Ferric chloride hexahydrate ($FeCl_3.6H_2O$, 98%) in a ratio of 1:1 volume (with a final concentration of 0.1M).

Both aqueous solutions were made using distilled deionized water. IONs were immediately obtained and the mixture was stirred for 60 min then, allowed

to stand at room temperature for another 30 min. The obtained colloidal suspension in both methods was centrifuged at 10000 rpm and washed several times with ethanol then dried at 40ºC under vacuum to obtain powdered IONs **(Mahdavi *et al*., 2013).**

Characterization of SIONs

Absorption measurements were carried out on UV-visible spectrophotometer (Specord Plus 210, analytic Jena) at a resolution of 1 nm, and in the range between 200–450 nm.

DLS measurement to the SIONs size in the colloids and their size distribution was done using the Malvern Zetasizer Instrument and the parameters were as follows: A laser wavelength of 633 nm (He–Ne), a scattering angle of 173◦ (fixed—without changing possibility), a measurement temperature of 25ºC, a medium viscosity of 0.8872 mPa.s and a medium refractive index of 1.330, and the material refractive index of 1.59. As an initial step, the colloid passed through a 0.2 m polyvinylidene fluoride (PVDF) membrane, then sample loaded into quartz microcuvette. Morphological analysis of the SIONs were carried out using TEM analysis at the Regional Center for Mycology and Biotechnology (RCMB), Al-Azhar University and the procedures was as follows: The biosynthesized SIONs was drop cast on carbon-coated copper grids and dried under vacuum desiccation and TEM micrographs of the sample were taken using the JEOL1010TEM instrument operated at an accelerating voltage of 200 kV. The crystallographic analysis of SIONs recorded using X-Ray Diffractometer Model: Xpert PRO with an accelerating voltage of 40 KV. The probable biomolecules which are responsible for reduction capping and effective stabilization of the SIONs recorded as follows: Samples mixed with potassium bromide at a ratio of 1:100. FTIR analysis was illustrated in the range of 500 to 4000cm $^{-1}$ using FTIR spectrophotometer (IRPrestige-21, Shimadzu Scientific, NODCAR) at diffuse reflectance mode.

Collection of *H. pylori* isolates

Thirty-six strains were isolated from gastric biopsies specimens from laboratories in some Egyptian hospitals (Cairo Governate, Egypt). These specimens were collected from October 2017 till December 2017 from dyspeptic

patients attending the Endoscopy Unit in those Egyptian hospitals. For bacterial culture, gastric biopsy samples were homogenized and cultured on Colombia blood agar plate (Oxoid, Basingstoke, UK) containing antibiotic supplement (vancomycin 6 mg/L, polymyxin-B 2500 IU/L, and amphotericin-B 2mg/L) with 7% horse blood. The plates were incubated at 37ºC in microaerophilic conditions (10% CO_2, 85% N_2, 5% O_2) and observed after 72 h. Organisms were identified as *H. pylori* based on colony morphology modified Gram staining, and positive oxidase, catalase, and rapid urease tests **(Van der Hulst *et al*., 1996; Mishra *et al*., 2002a and b).**

Antibiotics susceptibility test for *H. pylori*

Antimicrobial sensitivity of twenty-five *H. pylori* isolates was detected by agar disk-diffusion method. Bacterial suspension (McFarland tube no. 3) of *H. pylori* were inoculated on Mueller-Hinton Agar (MHA) (Oxoid, Basingstoke, UK) supplemented with 10% horse blood. The antibiotic disks of 6-mm diameter were purchased from (Oxoid, Basingstoke, UK) metronidazole (5µg), clarithromycin (15µg), levofloxacin (5µg), amoxicillin/clavulanic acid (20/10µg), tetracycline (30µg) and amoxicillin (10µg) were placed on the plates and incubated at 37ºC under microaerophilic conditions for 72 h .The inhibition zone diameter was measured in millimeters based on Clinical and Laboratory Standards Institute (CLSI) guidelines **(CLSI, 2018)**.

Determination of MIC by Agar Dilution Method

The minimum inhibitory concentration (MIC) was defined as the lowest concentration of antimicrobial agents inhibiting the visible bacterial growth. It was determined by the agar dilution method for each isolate **(CLSI, 2015)**. plates of MHA with aged (≥ 2 weeks old) horse blood (5% v/v) prepared by using two-fold dilutions of the antimicrobial agents; 200–0.0244µg/ml for amoxicillin, clarithromycin, and metronidazole. *H. pylori* suspensions prepared equal to (McFarland standard no. 2), and the inoculum (1-3µl per spot) plated directly on to the antimicrobial agent-containing agar dilution plates. Growth control plates free from antibiotics inoculated. All plates incubated at 37ºC for 72 h under microaerophilic conditions (10% CO_2, 85% N_2, 5%O_2) then MIC was recorded.

Molecular Identification of *H. pylori* using Hp1, Hp2 and Hp3

In this work, a Nested PCR approach has been used to detect *H. pylori* DNA. It was performed in two sequential amplification rounds using three oligonucleotide primers, Hp1, Hp2, and Hp3. positive control of DNA *H. pylori* SS1 and negative control of double-distilled water was used per each amplification in a thermal cycler (Gene Amp PCR System 9600, Perkin-Elmer, USA).

Primer sequences used in this study are as follows:

HP1(5'- CTGGAGAGACTAAGCCCTCC-3')

HP2 (5'- ATTACTGACGCTGATTGTGC-3')

HP3 (5'- AGGATGAAGGTTTAAGGATT-3')

The first amplification round was performed with a 5µl template DNA, 3µl Hp1 and Hp3 primers, 25µl Taq PCR master mix (2x), 17µl nuclease-free water. While the second amplification round was performed with a 1µl first amplification product, 3µl Hp1, and Hp2 primers, 15µl Taq PCR master mix (2x), 11µl nuclease-free water. The first and second amplification undergo the following procedures: 92ºC, 2 min; 50ºC, 2 min; 72ºC, 2 min; a final step at 72ºC, 4 min (35 cycles). The products of the second PCR, with an expected size of 109 bp, were visualized with 1.5% agarose gel electrophoresis at 100 V and ethidium bromide staining **(Cirak *et al*., 2003).**

Antimicrobial activity

Antimicrobial activity of SIONs was assessed against ten MDR *H. pylori*. SIONs suspension was prepared by using WAE, which mixed with Ferric chloride hexahydrate in the ratio of 1:1 and 2:1 (v/v). The assay was performed by plating the tested *H. pylori* on MHA supplemented with 5% horse blood. Wells were cut in MHA using a sterile cork-borer then100µl of SIONs solution for per each ratio was dispensed in each well. Control well was filled with ordinary WAE free from SIONs. Incubation was done at 37ºC under a microaerophilic condition for 24 h.

Inhibition zone diameter was measured in mm **(Van der Hulst *et al*., 1996; Thomas *et al*., 2012)**.

Furthermore, the MIC of SIONs against MDR *H. pylori* was detected. Pure bacterial cultures plated were used in MHA supplemented with 5% sterile horse blood for 24 h. SIONs were prepared in different concentrations (0.78 µg up to 400 µg) performed of two-fold dilution. Wells were cut in the plates using a sterile cork-borer and filled with 100µl of SIONs solution. Positive and negative controls were constructed and handled as experimental conditions. The plates were incubated for 24h at 37ºC under microaerophilic conditions **(Shanmugaiaha *et al*., 2015).** Zone of growth inhibition and MIC for each organism was recorded.

In order to explain the antibacterial mechanism of SIONs, TEM technique was used. Cells of *H. pylori* before and after treatment with nanoparticles were fixed overnight with 2.5% glutaraldehyde and drop coated on silicon wafers. Air-dried samples were sputter coated with gold and observed under TEM (JEOL 1010) **(Bozzola and Russell,1999)**.

Cytotoxic effect on human normal cell line using MTT assay

Cytotoxic effect on human normal epithelial cell line was measured using a microplate multi-well reader (Bio-Rad Laboratories Inc., Model 3350, Hercules, California, USA) at 595nm **(El-Menshawi *et al*., 2010).** Cell viability was assessed by the mitochondrial-dependent reduction of yellow MTT (3-(4,5-dimethylthiazol-2-yl)-2,5-diphenyl tetrazolium bromide) to purple formazan. The percentage of change in viability calculated according to the formula: [(Reading of extract / Reading of negative control) -1] x 100.

Statistical analysis

All tests were performed under sterile conditions in triplicate. Samples were presented as mean ± SD for three measurements. A statistical significance was tested between samples and negative control using independent t-test by SPSS 11 program. DMSO was used for dissolution of SIONs and its final concentration in the cells was less than 0.2% in MTT. Unpaired Student's t-test was used to calculate $P < 0.05$ for SIONs against the control. IC_{50} values were calculated using the dose-response curve.

Results and Discussion

Iron Oxide nanoparticles can be synthesized by using the biomass of *S. platensis* or even by using their water extract. The yellow ferric chloride solution changed to a colloidal dark brown solution as an indication of SIONs formation in the reaction mixture. UV-visible spectra of *S. platensis* AAB and WAE were recorded around290 nm due to surface plasma resonance of electrons and metal for both biosynthesized products which represented in Fig. (1). The UV-visible spectrophotometer analysis of the cell filtrate indicating the maximum absorbance with WAE solution at around 290 nm, which could be an indication for the transition of ferric chloride into SIONs. Our result agreed with **Das *et al*. (2014b) and Devatha *et al*. (2018)** who mentioned that IONs synthesized by *Azardirachta indica* and *Datura inoxia* leaf extracts indicated a peak at 296 nm and 270-290 nm, respectively.

Measurements using DLS figure out the stability of the colloidal suspensions, the hydrodynamic diameter as mean average and the size of nanoparticles **(Wiogo *et al*.,2011).** SIONs synthesized by using the WAE of *S. platensis* showed that the colloidal solution was stable because of the Poly Dispersity Index (PDI) which was equal to 0.334. These findings corroborate with the research done by **Demin *et al*. (2016)** who elucidated the stability of colloidal suspensions because of the PDI for NH_2-IONs were 0.22 and 0.29 with an average diameter of 160 nm and 140 nm, respectively. In another way, the SIONs synthesized by AAB of the *S. platensis* showed unstable colloidal suspension because of PDI value was equal to 0.662.

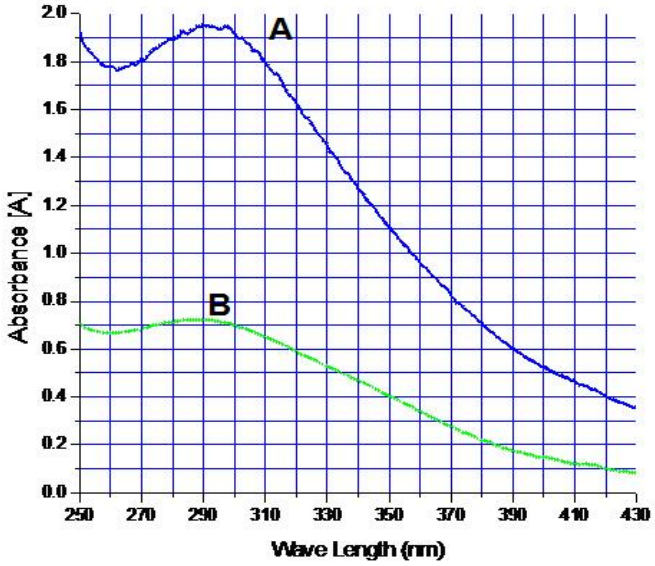

Fig.1. UV- vis absorption spectra of SIONs. A: SIONs biosynthesized by WAE, B: SIONs biosynthesized by AAB.

When PDI value is greater than 0.5, it means lower instability of the nanoparticles and their aggregation **(Masarudin *et al*., 2015).** Moreover, SIONs in the stable colloidal suspension showed an average size of 95.26 ± 23.8 nm representing by 86.2 % of the sample (Fig.2- curve A & B). Alternatively, SIONs in unstable colloidal suspension showed an average size of 221.2± 32.4 for 80% of the sample (Fig.2- curve C & D). Thus, this unstable suspension excluded from further analysis.

TEM images provided the morphology and accurate radius of particles which confirmed the rod-shape and uniform distribution without significant agglomeration of the SIONs (Fig.3 A & B). The analysis of data from TEM micrograph of SIONs showed that the particles length ranged from 99.15 nm to

165.16 nm, with an average length of 137.51 ±17.54nm. Figure.3 C illustrated that the frequency of SIONs length varied from 120-150 nm representing by 64%. While, the SIONs width ranged from 25.11nm to 54.47 nm, with an average width of 31.04 ±15.68 nm and their frequency varied from 30-45 nm by 68 % (Fig.3 D). The aspect ratio was calculated and ranged from 2.3 to 5.1 as illustrated in Table (1).

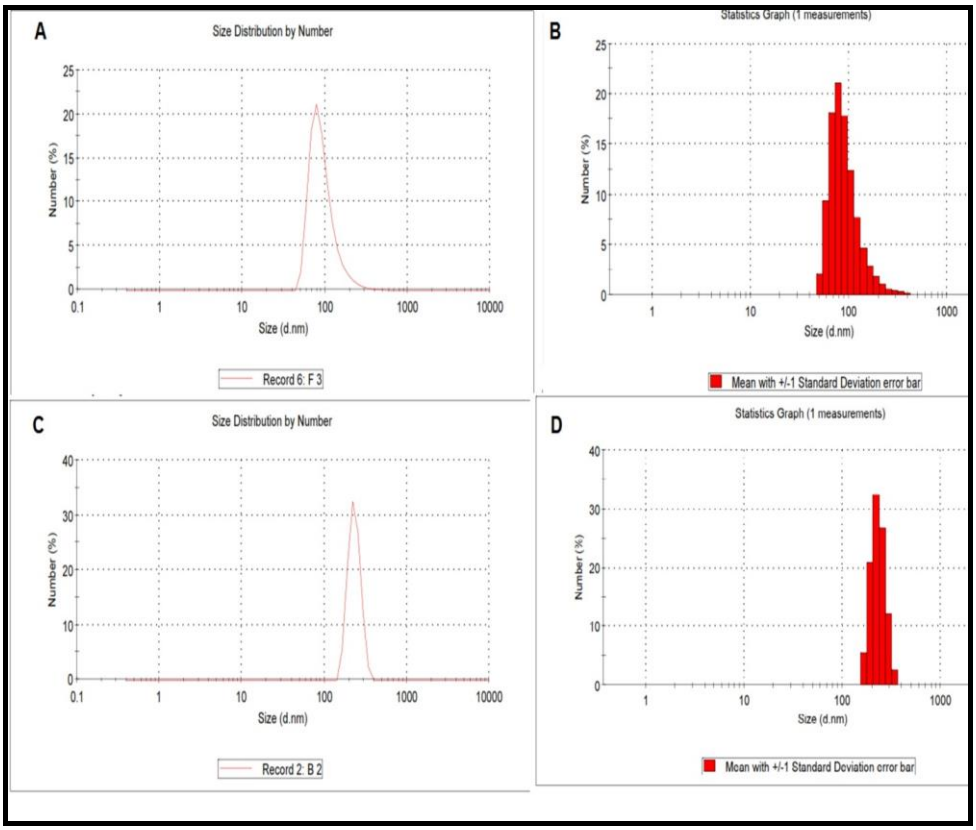

Fig.2. Size distribution of IONs by Dynamic Light Scattering (DLS) method for WAE (A) & their statistic graphs (B). Size distribution of IONs for AAB (C) and their statistic graphs (D).

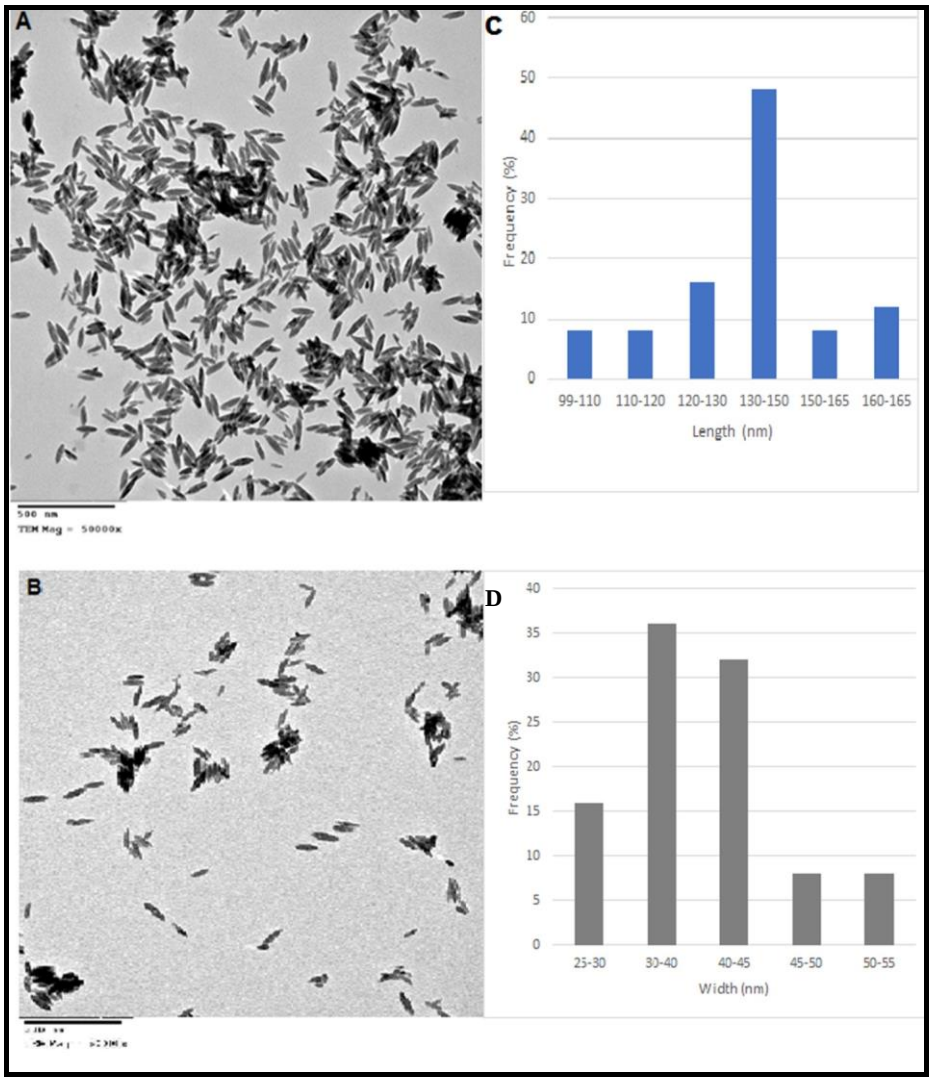

Fig.3 (A &B) TEM images of rod-shaped SIONs. (C&D): The frequency of length and width of rod-shaped SIONs respectively.

Table 1. Dimensions of rod-shape SIONs mean average using TEM.

Width ±15.68 nm	Length ±17.54 nm	Aspect ratio (Length/width)
53.65	125.94	2.3
34.67	135.26	3.9
40.95	125.68	3
33.25	144.46	4
33.69	165.16	4.9
25.11	99.15	3.9
41.67	148.41	3.5
29.34	145.05	4.9
42.55	147.48	3.4
27.37	139.63	5.1
25.70	132.65	5.1
33.69	164.56	4.8
39.00	155.25	3.9
45.33	133.05	2.9
40.49	162.38	4
35.41	134.02	3.7
40.95	110.30	2.69
43.07	129.40	3
41.67	128.48	3
54.47	143.82	2.64
47.57	148.31	3.1
29.34	108.95	3.7
31.76	139.20	4.3
33.14	157.44	4.7
32.80	113.78	3.4

The difference between DLS and TEM techniques explained in β FeOOH nanoparticles suggesting that rod-shaped nanoparticles moved by translational diffusion. The equal spherical hydrodynamic diameter of 62.33 nm proposes DLS outcomes with a single fixed angle of 173° overvalued the exact diameter where the length and width of the nanorods as 119.7 and 17.5 nm in TEM and this agrees with our present investigation **(Farrell *et al*., 2009; Lim *et al*., 2013).**

Our results using FTIR spectrum of dried *S. platensis* water extract and their corresponding SIONs showed strong absorption peaks at 3496, 3395.7, 2925, 2400.45, 1703, 1660.83, 1492.93, 1403, 1384.85, 1114.87, 880, 600 cm^{-1}as in Fig. 4 and Table (2). Infra-red spectrum displayed a frequency range from 3500–3200 cm^{-1} representing N-H stretching vibration due to proteins. A methylene group of proteins was represented at 2925 cm^{-1} peak, which, is considered as a signature peak. A peak at 1703 cm^{-1}attributes to C=O stretching of carboxylic acid. Peaks at 1660 $cm^{-1}$and 1492.93 cm^{-1}represent an amide I (C=O–) and amide II, respectively and this is a sign for protein components of *S. platensis*. 1403 cm^{-1}peak attributes to C-C stretching and vibration due to aromatic. 1384.85cm^{-1} presents in the N–O asymmetric stretching and vibration of nitrous compounds. The particular frequency ranges from 1250–1020 cm^{-1} C-N stretching, O-H vibration attributes to the presence of aliphatic amines. The frequency ranges from 910-665 cm^{-1} peaks are N-H wag stretching, vibration due to the presence of primary and secondary amines. The frequency ranges from 690–515 cm^{-1} peaks represent in C–Br stretching, vibration presence of alkyl halide compounds. Based on the above data, detection of a methylene group, amide I and amide II by FTIR confirm the presence of a protein group in the produced SIONs which agree with a previous study **(Das *et al*., 2010)**.

Also, detection of methylene group and amide I and amide II by FT-IR confirm the presence of protein group in the SIONs which, may have the major role as an antibacterial activity which agrees with other previous studies (**Das *et al*., 2014a; Devatha *et al*., 2018).**

Also, **Chronakes (2001)** mentioned that *Spirulina* sp. has a high protein percentage which ranges from 60% to 70%. It has high percentages of essential amino acids as Leucine, Valine, and Isoleucine. Denaturation of *S. platensis* noticed when heated above 67ºC and hydrogen bonds and hydrophobic regions formed during heating due to gelatin features of *S. platensis*

Upon this base, the probable mechanism for produced SIONs maybe is chelation between the carbonyl of the amide group in *S. platensis* extract which naturally exists and Fe^{+3} from ferric chloride hexahydrate added through the biosynthesis procedure as mentioned before. Finally, the formed IONs may be capped and stabilized with a protein chain of *S. platensis* extract. This explanation was agreed with IONs synthesized by *Datura* leaf extract **(Das *et al*., 2014b).**

XRD pattern of synthesized SIONs powder displayed in Fig.5. All diffraction peaks in this pattern had a good match with JCPDS cards no. 39-1346 which indexed to the cubic spinel phase of gamma ferric oxide (γ -Fe_2O_3 or maghemite). Small peaks agreed with peaks of the tetragonal phase of γ-Fe_2O_3 (JCPDS card no.25-1402) and magnetite (JCPDS card no.88-0315). The sample had distinctive peaks at position °2θ of 26.9, 31.8,35.2,39.3, 45.5,55.8, 56.6,61.3,64.3 and 84.1 and their corresponding relative intensity 69.4,100,55.5,27.3,46.7,26.8,29.9,9.7,11.7 and 7.5 respectively as in Table 3.

The incidence of bacterial antibiotic resistance appears to be obviously growing with time in many countries. In our study, A total of 36 specimens were collected from some Egyptian hospital laboratories. These specimens obtained from gastric biopsies of the antrum dyspeptic patients. Only 25 samples (69.5%) were identified as *H. pylori*. Identification was performed by testing for the presence of certain enzymes: oxidase, catalase, and urease after cultivation on the Colombia blood agar media under a microaerophilic condition then, microscopic observation was done for the Gram-negative curved rod morphology.

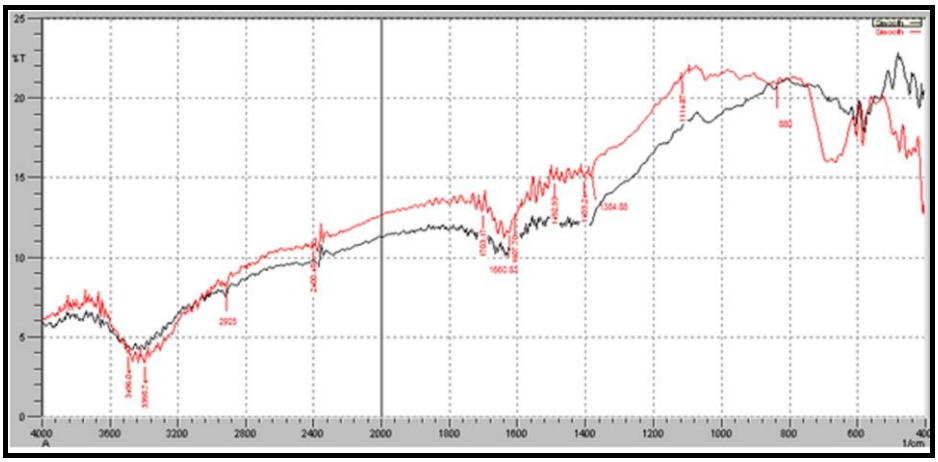

Fig.4. FTIR spectrum of dried WAE (red color) and SIONs (black color).

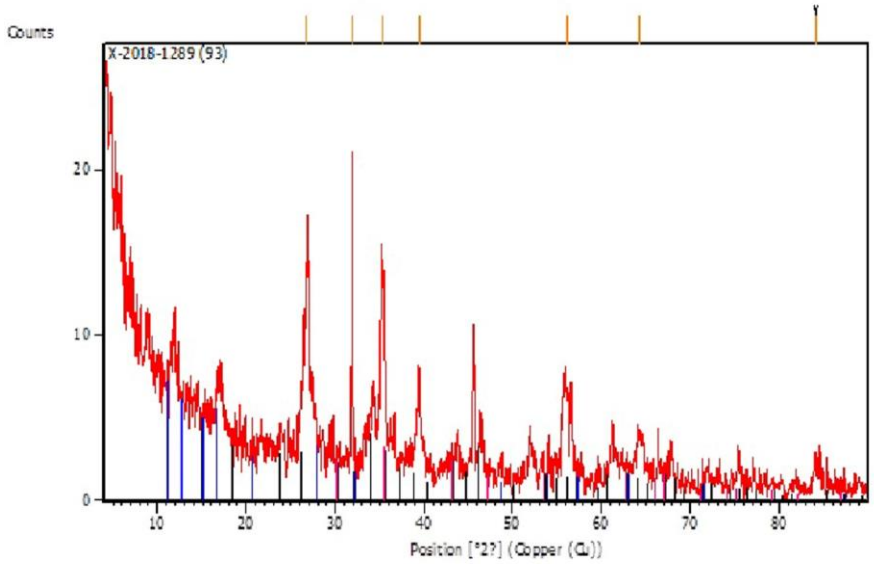

Fig.5. XRD pattern of SIONs (red color), cubic structure maghemite (black color, # 39-1346), tetragonal maghemite blue color, # 25-1402) and magnetite (pink color, # 88-0315).

Table 2. FT-IR Frequency range and the following functional groups present in WAE and SIONs.

Frequency (cm^{-1})	Frequency Ranges	Functional Groups
3496, 3395.7	3500-3200	N-H stretching vibration.
2925	3300-2500	Asymmetric stretching Alkanes (-CH2-).
1703	1700-1750	C=O stretching of carboxylic acids (esters or amino acids).
1660.83	1660-1620	Amide I (C=O–) stretching vibration.
1492.93	1480-1543(s)	(Amide II)
1403	1500-1400	C-C stretching vibration indication the presence of aromatic.
1384.85	1400-1290	N–O stretching vibration presence of nitro compounds.
1114.87	1250-1020	C–N stretching vibration presence of aliphatic amines.
880	910-665	N-H wag stretching vibration Presence of primary and secondary amines.
600	690-515	C–Br stretching vibration presence of alkyl halides.

Table 3. The °2θ, d values and intensities% of the peaks in the XRD pattern of SIONs.

Pos. [°2θ]	Height [cts]	FWHM* Left [°2θ]	d-spacing [Å]	Rel. Int. [%] **
11.8833	3.17	0.9446	7.44757	16.91
17.0354	2.74	0.9446	5.20498	14.62
26.9030	13.03	0.3149	3.31412	69.42
31.8262	18.77	0.1181	2.81180	100.00
35.2588	10.42	0.3936	2.54553	55.50
39.3763	5.12	0.6298	2.28832	27.30
45.5783	8.77	0.2362	1.99033	46.73
55.8602	5.03	0.4723	1.64592	26.81
56.6076	5.63	0.2362	1.62595	29.97
61.3072	1.82	0.9446	1.51210	9.70
64.3806	2.21	0.9446	1.44714	11.77
84.1897	1.42	0.9446	1.15003	7.55

(*) FWHM: Full width at half maximum.

(**) Rel. Int.: Relative intensity

Antimicrobial susceptibility test assessed for 25 *H. pylori* with different antibiotics. The maximum resistance was configured for amoxicillin/clavulanic acid with 13 isolates (52%). Whereas, the frequency of resistance to other antibiotics such as metronidazole, clarithromycin, and amoxicillin was recorded in 10 isolates (40%) which considered as MDR *H. pylori*. Only eight isolates (32%) were resistant to tetracycline. However, all tested isolates were sensitive to levofloxacin.

The MIC of metronidazole and clarithromycin against *H. pylori* was > 200µg/ml while, amoxicillin ≥200µg/ml which proved their high resistance. Our results agreed with **Mishra *et al.* (2006)** who reported the maximum resistance of metronidazole for 64% *H. pylori* isolates. Also, the resistance to metronidazole as high as 84% has been stated for African countries **(Glupczynsk *et al*.,1990)** but the mechanism of *H. pylori* resistance to metronidazole was not well identified **(Megraud,1998).** The MIC for amoxicillin > 256µg/ml recorded in one strain.

However, for clarithromycin and metronidazole were ≤48 µg/ml that quite differs from our results as mentioned by **(Mishra *et al*., 2006).**

Detection of 16S rRNA PCR assay confirmed that all the ten selected isolates were *H. pylori* and the PCR product was as expected at 109 bp (Fig. 6).Our results resembled a research done by Kargar and Doosti (2012) on 150 gastric biopsy samples for the presence of *H. pylori* using 16S rRNA PCR assay and the expected PCR product was also detected at 109 bp .

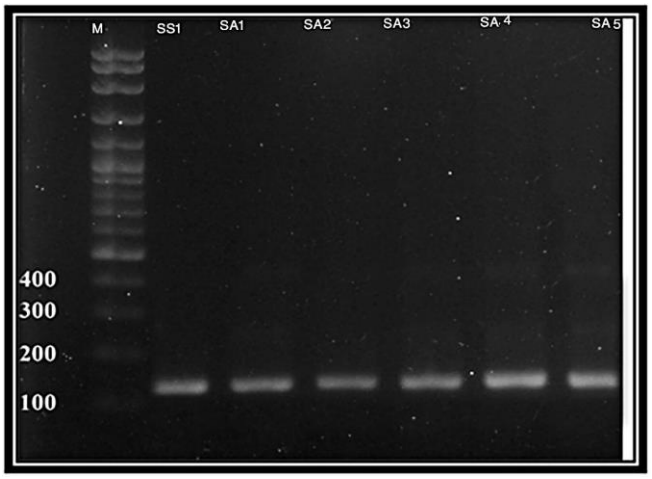

Fig.6: PCR amplification using Hp1, Hp2 and Hp3 detection for *H. pylori*, Lane (M) DNA molecular size marker (100bp) ladder, Lane (SS1) reference strain, and Lanes (SA1-SA5) representing *H. pylori* strains.

The antimicrobial efficacy of SIONs was assessed against MDR *H. pylori*. Our results showed that SIONs possess antibacterial activity by demonstrating a zone of inhibition which was more vivid in ratio 1:1 then ratio 1:2 in comparison to the control WAE free from SIONs (Fig.7 and 8).

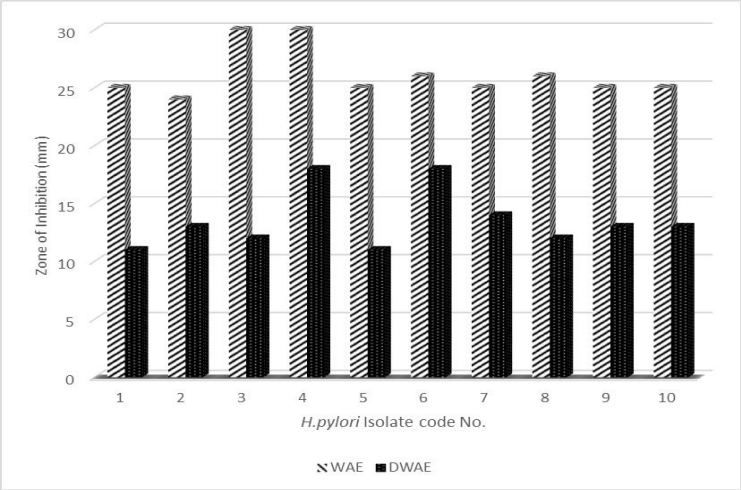

Fig.7. Screening for antibacterial activities of SIONs (from WAE &DWAE) against Multidrug-resistant *H.pylori.*

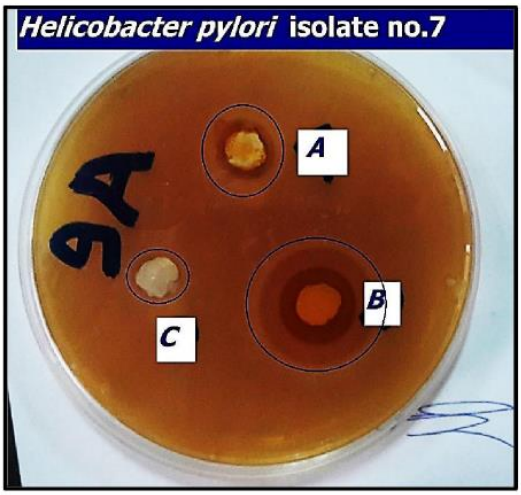

Fig.8. Antibacterial activities of SIONs synthesized using DWAE (A) and WAE (B) compared to control WAE free from SIONs (C) against MDR *H. pylori* isolate no.7

The MIC of SIONs was found to be 3.1 µg/ml for 80 % of MDR *H. pylori* and 12.5 µg/ml for the least isolates (20%). Antibacterial studies by metal oxide nanoparticles using a green approach are becoming more popular in the field of health aspects and drug production. The possible mechanism for the antibacterial activity of metal nanoparticles is an electromagnetic attraction between the positively charged nanoparticles and negatively charged bacteria. Once this attraction occurs, the bacteria become oxidized and die immediately **(Rezaei-Zarchi *et al*., 2010)**. Most ions released from nanoparticles react with –SH groups of the existing bacterial cell surface proteins which causes the cell decay **(Zhang and Chen, 2009)**.

Few studies demonstrated that IONs had a bactericidal effect on *S. epidermidis* as mentioned by **(Taylor and Webster, 2009).** It was hypothesized that the IONs with a high concentration could cause an electrostatic repulsion with negative bacteria surface leading to low antimicrobial activity. However, the positive potential IONs with low concentration had a strong interaction with the negative bacteria surface due to the oxidative stress by Reactive Oxygen Species (ROS) **(Arakha *et al*., 2015)**. ROS comprises radicals as superoxide radicals (O_2^-), hydroxyl radicals (–OH) and hydrogen peroxide (H_2O_2); and singlet oxygen ($^1O_2$) could be the cause of bacterial proteins destruction and DNA damage. ROS could have been produced by IONs leading to the inhibition of Gram-negative *Escherichia coli* and *Proteus vulgaris* **(Mahdy *et al*., 2012; Prabhu and Rao, 2015)**.

The effect of SIONs on the *H. pylori* morphology was evaluated using TEM as observed in (Fig.9-I). The normal bacterial cell was undamaged and undergo binary fission. However, after treatment with SIONs, structural changes and major damage in the morphology was clearly observed by TEM micrograph (Fig.9A-H). Our observations confirmed the deformation of the cell wall, membrane fragmentation, complete disruption and leakage of bacterial components.

Cytotoxic activity test by MTT assay measurement was performed in vitro to demonstrate cytotoxicity and cell proliferation upon quantifying cell viability. In the present investigation, no cytotoxic effect detected for SIONs at all tested concentrations which ranged from 100 to 0.78 µg/ml on the human epithelial cell line. Our cytotoxicity examination revealed safe use of SIONs which may be due

to the presence of positively charged amino groups in protein coating SIONs as figured out in FTIR analysis. Moreover, TEM analysis demonstrated that the mean average length and width for SIONs were 137.51 and 31.04 nm, respectively which considered relatively large in size. Our result agreed by **Ying and Hwang (2010)** and **Guichard *et al*. (2012)** who explained that Nano- and sub-micro-sized IONs did not significantly produce intracellular reactive Oxygen Species (ROS) due to the surface charge of nanoparticle and their sizes. The smaller size of IONs was found more cytotoxic than those of larger size. Moreover, carboxyl-coated IONs caused higher cytotoxicity in comparison with amine-coated IONs.

Conclusion

To our knowledge, the present study is the first report on the synthesis of SIONs using cyanobacterium *Spirulina platensis.* The biosynthesized of SIONs could efficiently inhibit Multi-Drug Resistant *Helicobacter pylori.* This investigation requires a vivo application on the SIONs as a possible, safe and eco-friendly pharmaceutical product to eradicate experimentally the MDR *H. pylori*.

Acknowledgments

We acknowledge the physical chemistry laboratory at NODCAR for FTIR analysis used in this study.

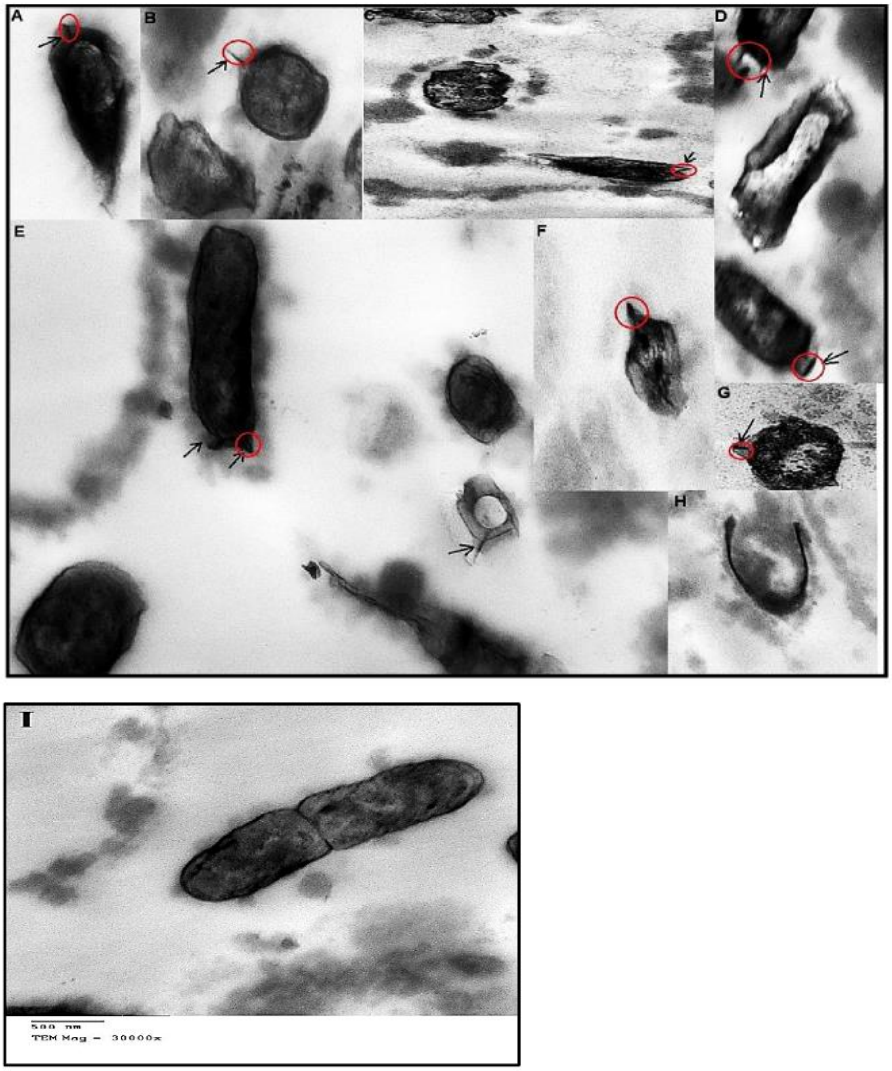

Fig.9. TEM images (A, B, C, D, E, F, G, and H) of *H. pylori* after treatment with MIC_{50} of SIONs showed cell wall deformation and destruction for cell membrane and finally complete death of bacteria compared to normal *H. pylori* without any treatment showed binary fission (I).

References

Achmadi S.S. and Tri-Panji S. (2000). Pemanfaatan limbah lateks pekat sebagai media pertumbuhan ganggang mikro *Spirulina platensis* pemghasil asam γ-linoleat. Bogor, Unit Penelitian Bioteknologi Perkebunan, *Laporan Riset Unggulan Terpadu* (RUT)V,**1997-1999. 32.**

Ahmed E.A., Abdel Hafez E.H., Ismail A.F.M., El Sonbaty S.M., AbbasH.S. and Salah El Din R.A. (2015). Biosynthesis of Silver Nanoparticles by *Spirulina platensis* & *Nostoc* sp., *Glob. Adv. Rese. J. Microbiol.* IV.**4, 36-49.**

Ali M.I., Sharma G., Kumar M.A., Jasuja N.D. and Rajgovind I. (2015). Biological Approach of Zinc Oxide Nanoparticles Synthesis by Cell-Free Extract of Spirulina platensis. *Int. J. Curr. Eng. Tech.***5**, **2531-2534.**

Arakha M., Pal S., Samantarrai D., Panigrahi T.K., Mallick B.C., Pramanik K., Mallick B.and Jha S. (2015). Antimicrobial activity of iron oxide nanoparticle upon modulation of nanoparticle-bacteria interface. *Sci. Rep.***5**, **1-12.**

Berry A. and Curtis A.S.G. (2003). Functionalization of Magnetic Nanoparticles for Applications in Biomedicine. *J. Phys.***36**, **198-206**. doi:10.1088/0022-3727/36/13/203.

Bozzola J.J., and Russell D.L. (1999). Electron microscopy: Principles and Techniques for Biologists, 2nd Ed., Jones and Bartlett Publishers.**670p**.

Chronakes I.S. (2001). Gelation of edible blue-green algae protein isolates (*Spirulina platensis*): Thermal transitions, archeological properties, and molecular forces involved. *Bioresour Technol*. **77**, **19-24**.

Cirak Y.M., Ozdek A., Yilmaz D., Bayiz U., Samim E. and Turet S. (2003). Detection of *Helicobacter pylori* and Its CagA Gene in Tonsil and Adenoid Tissues by PCR. *Arch Otolaryngol. Head Neck Surg.***129**, **1225-1229**.

CLSI. (2015). Methods for Antimicrobial Dilution and Disk Susceptibility Testing of Infrequently Isolated or Fastidious Bacteria. 3rd ed. CLSI guideline M45. Wayne, PA: Clinical and Laboratory Standards Institute.

CLSI. (2018). Clinical and Laboratory Standards Institute. Performance standards for antimicrobial susceptibility testing: CLSI Guideline M100-S28; Wayne, PA: Clinical and Laboratory Standards Institute.

Das R.K., Borthakur B.B. and Bora, U. (2010). Green synthesis of gold nanoparticles using ethanolic leaf extract of *Centella asiatica*. *Mater. Lett*. 64, **1445–1447.**

Das A. K., Marwal A. and Verma R. (2104a). Bio-reductive Synthesis and Characterization of Plant Protein Coated.Magnetite Nanoparticles**.** *NanoHybrids*.2; Vol. **7. 69-86.**

Das A.K., Marwal A. and Verma R. (2014b). *Datura Inoxia* Leaf Extract Mediated One Step Green Synthesis and Characterization of Magnetite (Fe_3O_4) Nanoparticles. *J. Pharm. Nanotechnol.* **2**, **21-24.**

Demin A.M., Pershina A.G., Ivanov V.V., Nevskaya K.V., Shevelev O.B.,Minin A.S., Byzov I.V., Sazonov A.E., **Krasnov V.P. and Ogorodova L.M.** (2016). 3-Aminopropylsilane-modified iron oxide nanoparticles for contrast-enhanced magnetic resonance imaging of liver lesions induced by *Opisthorchis felineus*. *Int. J. Nanomedicine*.**11, 4451–4463.**

Devatha C.P., Jagadeesh K. and Patil M. (2018).Effect of Green synthesized iron nanoparticles by *Azardirachta Indica* in different proportions on antibacterial activity. *ENMM*. **9**, **85-94.**

El-Menshawi, B.S., Fayad, W., Mahmoud, K., El-Hallouty, S.M., and El-Manawaty Olofsson M.H. and Linder S.(2010). Screening of natural products for Therapeutic activity against solid tumor. *IJEB***.48, 258-264.**

Farokhzad, O.C. and Langer, R. (2009). Impact of nanotechnology on drug delivery. *ACS Nano*.**3**, **16-20**.

Farrell D., Dennis C.L., Lim J.K. and Majetich S.A. (2009). Optical and electron microscopy studies of Schiller layer formation and structure. *J of Colloid Interface Sci.* **331**, **394–400.**

Glupczynski Y., Burette A. and DeKoster E. (1990). Metronidazole resistance in *Helicobacter pylori*. *Lancet*. **338**, **976–977.**

Guichard Y., Schmit J. and Darne C. (2012). Cytotoxicity and genotoxicity of nanosized and microsized titanium dioxide and iron oxide particles in Syrian hamster embryo cells. *Ann. Occup. Hyg.***56**, **631–644**.

Guoa J., Wanga J., Tjiu R. W.W., Pan J. and Liu T. (2012). Synthesis of Fe nanoparticles and graphene composites for environmental applications. *J. Hazard. Mater*. **225–226, 63–73.**

Hasany S.F., Ahmed I., Rajan, J. and Rehman A. (2012). Systematic Review of the Preparation Techniques of Iron Oxide Magnetic Nanoparticles *J. Nanosci.Nanotechnol*.**2**, **148-158.**

Kargar M. and Doosti A. (2012). Detection of four clarithromycin resistance point mutations in Helicobacter pylori: comparison of real-time PCR and PCR-RFLP methods. *Comp Clin Pathol* ; **22(5):1-7.**

Li J. and Perez-Perez G.I. (2018). *Helicobacter pylori* the latent Human Pathogen or Ancestral Commensal Organism. *Front Microbiol*.**9**, **609**; doi: 10.3389/fmicb.2018.00609.

Lim J., Yeap S.P., Che H.X. and Low S.C. (2013). Characterization of magnetic nanoparticle by dynamic light scattering. *Nanoscale Res. Lett*.**8**, **1-14.**

Mahdavi M., Namvar F., Ahmad M. and Mohamad R. (2013). Green Biosynthesis and Characterization of Magnetic Iron Oxide (Fe_3O_4) Nanoparticles Using Seaweed (*Sargassum muticum*) Aqueous extract. *Molecules*. **18**, **5954-5964**.

Mahdy S.A., Raheed Q.J. and Kalaichelvan P.T. (2012). Antimicrobial activity of zero-valent iron nanoparticles. *Int. J Mod. Eng. Res.***2**, **578–581**.

Masarudin M.J., Cutts S.M., Evison B.J., Phillips D.R. and Pigram B.J. (2015). Factors determining the stability, size distribution, and cellular accumulation of small, monodisperse chitosan nanoparticles as candidate vectors for anticancer drug delivery: application to the passive encapsulation of [14C]-doxorubicin. *Nanotechnol. Sci. Appl.***8**, **67–80.**

Megraud F. (1998). Epidemiology and mechanism of antibiotic resistance in *Helicobacter pylori*.*Gastroenterol.* **115**, **1278–1282.**

Megraud F. and Lehours P. (2007). *Helicobacter pylori* detection and antimicrobial susceptibility testing. *Clin. Microbiol. Rev.***20**, **280-322.**

Mishra K.K., Srivastava S., Dwivedi P.P., Prasad K.N. and Ayyagari, A. (2002a). ureC PCR of cagA gene-based diagnosis of *Helicobacter pylori* infection and detection gastric biopsies. *Ind. J. Pathol. Microbiol.***45**, **31–38.**

Mishra K.K., Srivastava S., Dwivedi P.P., Prasad K.N. and Ayyagari, A. (2002b). Genotype of *Helicobacter pylori* isolated from various acid peptic diseases in and around Lucknow.*Curr Sci*.**83**, **749–755.**

Mishra K.K., Srivastava S., Garg A. and Ayyagari A. (2006). Antibiotic Susceptibility of *Helicobacter pylori* Clinical Isolates: Comparative Evaluation of Disk-Diffusion and E-Test Methods. *Curr. Microbiol*.**53**, **329–334**.

Prabhu Y.T. and Rao K.V. (2015). Synthesis of Fe_3O_4 Nanoparticles and its Antibacterial Application. *Int. Nano. Lett*.**5**, **85–92.**

Rezaei-Zarchi S., Javed A., Ghani M.J., Soufian S., Firouzabadi F.B., Moghaddam A.B. and Mirjalili S.H. (2010). Comparative study of antimicrobial activities of TiO_2 and CdO nanoparticles against the pathogenic strain of *Escherichia coli*. *Iran J. Pathol*.**5**, **83–89.**

Shanmugaiaha V., Harikrishnana H., Al-Harbib S.N., Shineb K., Khaled J.M. and Balasubramaniance N. (2015). Facile synthesis of silver nanoparticles using *Streptomyces* sp. vsmgt1014 and their antimicrobial efficiency. *Dig. J. Nanomater. Biostruct.* **10**, **179-187**.

Sharma P.K. and Bhandari R. (2006). High-light-induced Changes on photosynthesis, pigments, sugars, lipids and Antioxidants Enzymes in fresh water (*Nostoc Spongiaforme*) and marine (*Phormidium corium*) Cyanobacteria. *J.Photochem. Photobio.***82**, **702-710**.

Slonczewski L., John L. and John W.F. (2009). Microbiology: An Evolving Science. 2nd Ed. New York: W.W. Norton &Company, Inc., **141-685**.

Taylor E.N. and Webster T.J. (2009). The use of superparamagnetic nanoparticles for prosthetic biofilm prevention. *Int. J. Nanomedicine*. **4**,**145–152**.

Thamphiwatana, S. (2014). Antimicrobial Nanotherapeutics Against Helicobacter pylori Infection. Ph.D. thesis, Nanoengineering, University of California, San Diego. Publication Number: AAT 3639270; ISBN: 9781321235760; Source: Dissertation Abstracts International, Volume: 76-02(E), Section: B.; 168 p.**1-2**.

Thomas R., Viswan A., Mathew J. and Radhakrishnan E.K. (2012). Evaluation of Antibacterial Activity of Silver Nanoparticles Synthesized by a Novel Strain of Marine *Pseudomonas* sp. *Nano. Biomed. Eng*.**4**,**139-143**.

Van der Hulst R.W.M, Verheul S.B., Weel J.F.L., Gerrits Y., and Tenkate F.J.W., Dankert J. and Tytgat G.N.J. (1996). Effect of Specimen Collection Techniques, Transport Media, and Incubation of Cultures on the Detection rate of *Helicobacter pylori*. *Eur. J. Clin. Microbiol. Infect. Dis.***15**:**211–215**.

Wiogo H.T.R., Lim M., Bulmus V., Yun J. and Amal R. (2011). Stabilization of magnetic iron oxide nanoparticles in biological media by fetal bovine serum (FBS). *Langmuir*.**27**:**843–850.**

Ying E. and Hwang H-M. (2010). In vitro evaluation of the cytotoxicity of iron oxide nanoparticles with different coatings and different sizes in A3 human T lymphocytes. *Sci.Total Environ.***408**:**4475–4481**.

Zhang H. and Chen G. (2009). Potent antibacterial activities of Ag/TiO_2 nanocomposite powders synthesized by a one-pot sol-gel method. *Environ. Sci. Technol*.**43**: **2905–2910.**

توصيف الجسيمات النانويه لأكسيد الحديد الأسبيروجين ونشاطها في تطورعلاج بكتريا الهليكوباكتر بيلورى المقاومة للمضادات الحيوية

شيرين محمد أشرف شرف , هبه صلاح عباس , طارق عبد المنعم اسماعيل

قسم الميكروبيولوجي-هيئه الرقابة والبحوث الدوائية

لقد تمت هذه الدراسة على نانو أكسيد الحديد الأسبيروجين المنتج من المستخرج المائى لطحلب الأسبيرولينا وقد تم الأنتاج بطريقة بسيطة وسريعة وآمنه بالجمع بين كلوريد الحديديك مع إستخراج المياه من الأسبيرولينا بلانتينزيس (Spirulina platensis) وقد أجرى إختبار التحليل الطيفى بإستخدام الأشعة فوق البنفسجية على مقياس 290 نانومتر.

كما تم استخدام المجهر الالكترونى النافذ لتسجيل شكل مقاييس الجزيئات بمعدل عرض 31.04 ومعدل طول 137.51 نانومتر. كما أظهرت الأشعة السينية أن أكسيد الحديد النانوى هو نوع من(ميجاميت) مكعب فى المرحلة الحلزوني جاما وعلاوة على ذلك, فقد أظهر أكسيد الحديد النانوى الأسبيروجين نشاط جيد كمضاد لبكتيريا الهليكوباكتر بيلورى المقاومة للعقاقير المتعددة. وقد أظهرت الدراسة أن الحد الأدنى لتركيز الجسيمات النانويه المنتجة في مقاومة تلك البكتريا قد سجلت3.1 ميكروجرام/ملليجرام, فى حين أظهر المجهر الألكتروني النافذ صور للخلايا البكتيرية وتمزقها وتسرب محتويات الخلية وتفتت الغشاء الخارجي لها بعد تعرضها لماده أكسيد الحديد النانوى الأسبيروجين.وقد أجرى إختبار نشاط السمية الخلوية لمنتج أكسيد الحديد النانوى على الخلايا الخلوية حيث كشفت النتائج أنة منتج آمن ويمكن إستخدامه بفاعلية كمنتج طبيعي .

كما وجد ان إستخدام طحلب الأسبيرولينا بلاتينزسيز كمصنع لإنتاج وعمل نانو اكسيد الحديد يمكن أن يكون له دور مستقبلي فى علاج الإصابة ببكتريا الهيلكوباتر بيلورى.